Phase diagram of the strongly disordered s-wave superconductor NbN close to the metal-insulator transition

Madhavi Chand,[1] Garima Saraswat,[1] Anand Kamlapure,[1] Mintu Mondal,[1] Sanjeev Kumar,[1] John Jesudasan,[1]
Vivas Bagwe,[1] Lara Benfatto,[2] Vikram Tripathi,[1] and Pratap Raychaudhuri[1,*]

[1]*Tata Institute of Fundamental Research, Homi Bhabha Road, Colaba, Mumbai 400005, India*
[2]*ISC-CNR and Department of Physics, Sapienza University, Piazzale Aldo Moro 5, 00185 Rome, Italy*

We present a phase diagram as a function of disorder in three-dimensional NbN thin films as the system enters the critical disorder for destruction of the superconducting state. The superconducting state is investigated using a combination of magnetotransport and scanning tunneling spectroscopy measurements. Our studies reveal three disorder regimes. At low disorder ($k_F l \sim 10$–4), the system follows the mean field Bardeen-Cooper-Schrieffer behavior, where the superconducting energy gap vanishes at the temperature at which electrical resistance appears. For stronger disorder ($1 < k_F l < 4$), a "pseudogap" state emerges, where a gap in the electronic spectrum persists up to temperatures much higher than T_c, suggesting that Cooper pairs continue to exist in the system even after the zero resistance state is destroyed. Finally, at even stronger disorder ($k_F l < 1$), the global superconducting ground state is destroyed even though superconducting correlations continue to survive, as evidenced from a pronounced magnetoresistance peak at low temperatures.

I. INTRODUCTION

In recent years, the effect of strong disorder in conventional s-wave superconductors has attracted renewed attention, motivated by the observation of novel electronic phases close to the critical disorder at which superconductivity gets destroyed. In the low-disorder limit, based on Bardeen-Cooper-Schrieffer (BCS) theory, Anderson[1] postulated that the superconducting transition temperature T_c of a superconductor will remain unchanged. However, subsequent measurements on a variety of systems[2–8] showed that as the disorder level is increased toward the strong disorder limit, T_c gradually decreases, eventually leading to a nonsuperconducting ground state. It is now understood that superconducting correlations continue to play a dominant role in the electronic properties even after the global superconducting ground state is destroyed. These correlations manifest through several phenomena: a giant peak in the magnetoresistance in strongly disordered superconducting films,[9–13] the persistence of magnetic flux quantization in strongly disordered Bi films even after the film is driven into an insulating state,[14] finite high-frequency superfluid stiffness above the superconducting transition temperature,[15] and more recently, the observation of a pronounced "pseudogap" in the electronic spectra of several strongly disordered superconductors,[16–18] which persists up to temperatures many times T_c. These observations lead to the obvious question of whether strong disorder can destroy the superconducting state without suppressing the underlying pairing interactions, leading to electronic states with finite Cooper pair density but no global superconductivity.

The suppression of superconductivity in the presence of strong disorder is driven by two distinct, but not mutually exclusive, effects. The first effect results from the increase in electron–electron (e-e) Coulomb repulsion caused by a loss of effective screening,[19,20] which partially cancels the electron–phonon–mediated attractive pairing interaction. The second effect comes from the decrease in superfluid density n_s induced by disorder scattering[21] in the presence of strong disorder.

Because reduced n_s and loss of effective screening both render the superconductor susceptible to quantum and classical phase fluctuations,[22] enhanced phase fluctuations can destroy the superconducting state even when the pairing amplitude remains finite.[23] Although both of these mechanisms have been invoked to explain different sets of experimental observations, a hierarchical scheme to understand the relative importance of these effects at different levels of disorder is at present lacking.

In this paper, we address this issue through a combination of magnetotransport and tunneling measurements on three-dimensional (3D) NbN thin films (with thicknesses much larger than the dirty limit coherence length ξ) grown through reactive magnetron sputtering. The disorder is tuned by controlling the level of Nb vacancies in the lattice, which is controlled by changing the Nb/N ratio in the plasma. For each film, we characterize the effective disorder through $k_F l$, where l is the electronic mean free path and k_F is the Fermi wave vector. The disorder in this set of films spans a wide range, from the moderately clean limit ($k_F l \sim 10$) down to $k_F l \sim 0.4$. Consequently, the normal state resistivity ρ at low temperatures varies by five orders of magnitude and T_c ranges from 17 K in the cleanest sample to <300 mK for the samples with $k_F l < 1$. Our study reveals three regimes: At moderate disorder ($10 > k_F l > 4$), T_c starts getting gradually suppressed but the system continues to follow conventional BCS behavior, where the superconducting energy gap disappears at the temperature at which resistance appears. For stronger disorder ($4 > k_F l > 1$), a "pseudogap" state emerges, where a gap in the electronic energy spectrum persists up to a temperature $T^* \gg T_c$. Finally, at even stronger disorder ($k_F l < 1$), we obtain a nonsuperconducting state, characterized by a pronounced peak in the magnetoresistance at low temperatures. Based on these observations, we construct a phase diagram that clearly delineates the relative importance of different mechanisms at different levels of disorder.
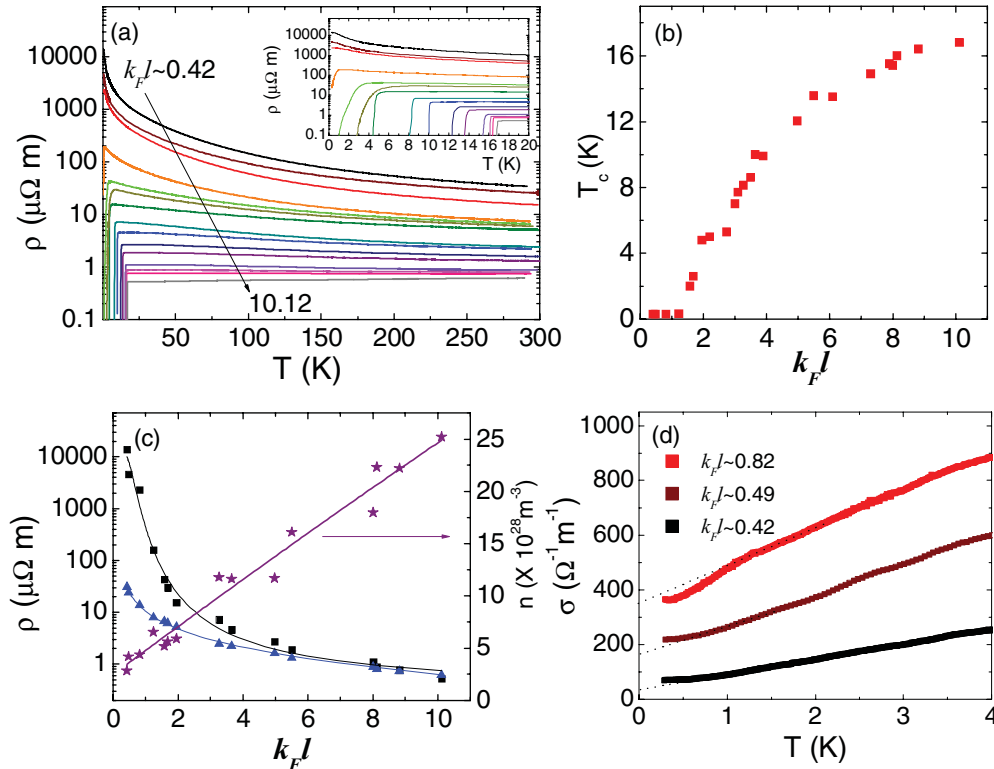
FIG. 1. (Color online) (a) ρ vs T for NbN films with different $k_F l$; the inset shows the expanded view at low temperatures. (b) Variation of T_c with $k_F l$. (c) Variation of n (purple stars), $\rho(285 \text{ K})$ (blue triangles) and ρ_m (black squares) with $k_F l$. (d) Conductivity σ vs T at low temperature for the samples with $k_F l \sim 0.82$, 0.49, and 0.42. The dotted lines are extrapolations to $\sigma(T \to 0)$.

II. EXPERIMENTAL DETAILS

Epitaxial thin films of NbN were grown using reactive magnetron sputtering on (100)-oriented single crystalline MgO substrates, by sputtering a Nb target in an Ar/N$_2$ gas mixture. The thickness of all of our films, measured using a stylus profilometer, was $\gtrsim 50$ nm, which is much larger than the dirty-limit coherence length[24] ($\xi \sim 4$–8 nm) in the superconducting state. Thus, from the point of view of superconducting fluctuations, all of our samples are effectively in the 3D limit. The effective disorder, resulting from the number of Nb vacancies in the NbN crystalline lattice, was controlled by controlling the sputtering power and/or the Ar/N$_2$ gas ratio, both of which effectively changed the Nb/N ratio in the plasma. Details of synthesis and structural characterization of the films have been reported elsewhere.[25–27]

Resistance R, magnetoresistance MR $= [\rho(H) - \rho(0)]/\rho(0)$, and Hall effect measurements were performed using standard four-probe techniques from 285 K down to 300 mK using a conventional ^{4}He or ^{3}He cryostat up to a maximum field of 12 T. For each film, $k_F l$ was determined from ρ and the Hall coefficient R_H measured at 285 K using the free electron formula $k_F l = \{(3\pi^2)^{2/3}\hbar[R_H(285 \text{ K})]^{1/3}\}/[\rho(285\text{K})e^{5/3}]$, where $\hbar$ is Plank's constant and e is the electronic charge. R_H was calculated from the Hall voltage deduced from reversed field sweeps from 12 to -12 T after subtracting the resistive contribution. Although in a noninteracting scenario $k_F l$ could provide a unique measure of electronic disorder, e-e interactions can significantly alter this scenario. We therefore calculate $k_F l$

from R_H and ρ measured at the highest temperature of our measurements (285 K), where the effect of e-e interactions is expected to be small.[28] The upper critical field H_{c2} for several samples was measured from either $\rho(T)$–T scans at different magnetic fields H or $\rho(H)$–H scans at different temperatures (with H perpendicular to the plane of the film).

Scanning tunneling spectroscopy (STS) measurements were performed using a home-built, high-vacuum, low-temperature scanning tunneling microscope[29] (STM) operating down to 2.6 K. The samples used in STS measurements were grown *in situ* in a sputtering chamber connected to the STM. A pair of horizontal and vertical manipulators was used to transfer the sample from the growth chamber to the STM without exposing it to air. The tunneling density of states (DOS) was extracted at various temperatures from the measurement of tunneling conductance $(G(V) = (\frac{dI}{dV}))$ as a function of voltage V between the sample and a Pt-Ir tip using a lock-in–based voltage modulation technique operating at 312 Hz and a modulation voltage of 100 μV.

III. RESULTS

We first summarize the evolution of the zero field transport properties with disorder. Figure 1(a) shows ρ–T for NbN films, with $k_F l$ ranging from 10.12 to 0.42. All samples, other than the one with $k_F l \sim 10.12$, show a negative temperature coefficient[26] of ρ. For samples with $k_F l > 1$, T_c (defined as the temperature at which resistance reaches 1% of its normal state value) varies from 16 K to <300 mK with increasing disorder.
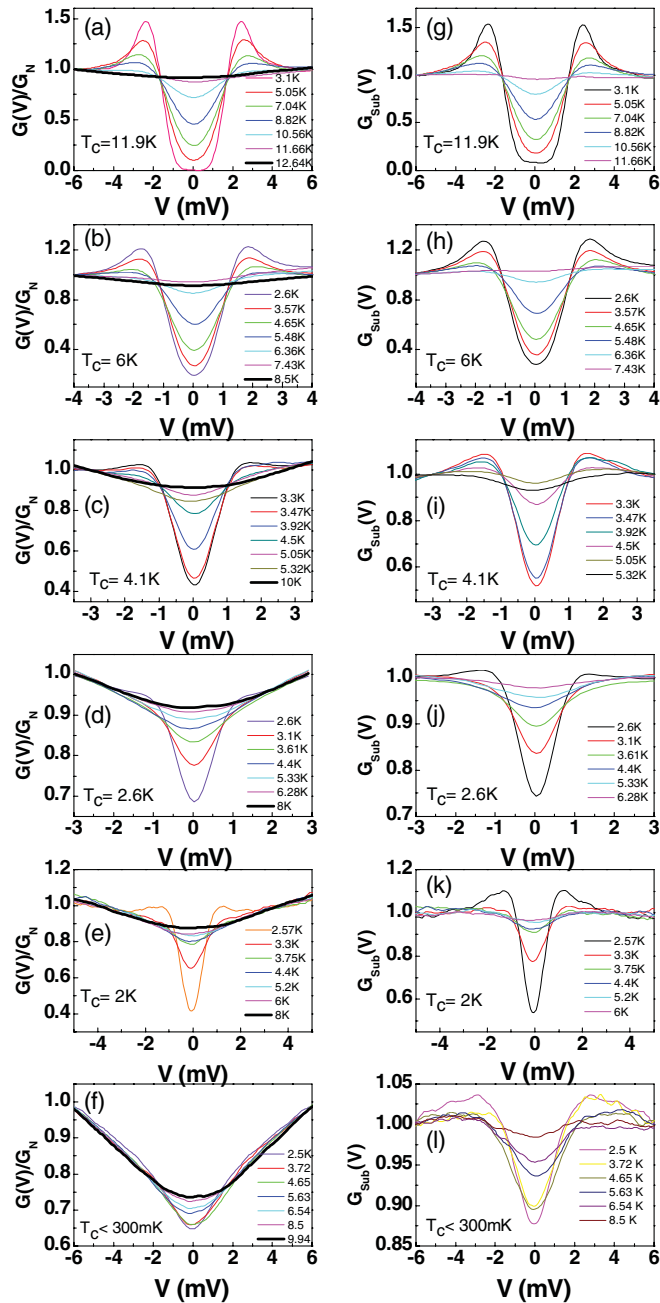
FIG. 2. (Color online) (a)–(f) Normalized tunneling spectra at different temperatures for NbN films with different levels of disorder. The spectrum shown in the thick line corresponds to the temperature at which the low-bias feature in the tunneling conductance disappears. Each tunneling spectrum is averaged over 32 equally spaced points along a 150 nm line on the sample surface. (g)–(l) The spectra corresponding to (a)–(f) after subtracting the V-shaped background.

The samples with $k_F l < 1$ remain nonsuperconducting down to 300 mK. Figure 1(b) shows the variation of T_c with $k_F l$. We observe that $T_c \to 0$ as $k_F l \to 1$. The carrier density n at 285 K ($n = 1/e R_H$(285 K)) and the normal state resistivity ρ(285 K) for all samples are shown in Fig. 1(c). In the same graph, we also plot the maximum resistivity ρ_m (taken as the peak value of ρ before the onset of the superconducting transition for $k_F l > 1$ and ρ at 300 mK for $k_F l < 1$), which varies

by five orders of magnitude from 0.5 to 15 000 $\mu\Omega$ m over the entire range of disorder. In this context, although $k_F l \sim 1$ is usually associated with the Anderson metal–insulator transition, such a classification is not straightforward in a disordered electronic system, where e-e interactions can play a significant role. For our films with $k_F l < 1$, the conductivity ($\sigma = 1/\rho$) increases linearly with temperature [Fig. 1(d)] and shows a small positive intercept when extrapolated to $T \to 0$, typical of a "bad" metal.[3,30] In our opinion, the bad metallic behavior observed for $k_F l < 1$ reflects the inaccuracy associated with the determination of this parameter based on a free-electron formula in a system where e-e interactions arising from the diffusive motion of the electrons could be important. We have observed remarkable consistency among ρ_m, T_c, and n for different films grown over a period of more than two years.

To explore the superconducting state, STS measurements were performed on several films with different levels of disorder. The measurement was performed by recording $G(V)$ vs V on 32 equally spaced points along a 150 nm line at different temperatures, which allowed us to obtain information on both the temperature evolution and the spatial variation of the tunneling DOS in the sample. Figures 2(a)–2(f) show the normalized conductance $G(V)/G_N$, where $G_N = G(V \gg \Delta/e)$, as a function of V, averaged over the 32 points, at different temperatures for six samples with different levels of disorder. For the first three samples [Figs. 2(a)–2(c)], where the lowest temperature of measurement is less than T_c, the conductance spectra show a dip at $V = 0$ and two symmetric peaks as expected from BCS theory. This feature is also observed in the next two disordered samples [Figs. 2(d) and 2(e)], where the lowest temperature of our measurements is higher than T_c. The most disordered sample ($T_c < 300$ mK) shows a dip in $G(V)$ for $V \lesssim 2$ mV, which rides over a broader V-shaped background that extends up to high bias. This nearly temperature–independent broad background is observed for all of our samples and persists up to the highest temperature of our measurements. It arises from Altshuler-Aronov–type e-e interactions and becomes more pronounced for samples with higher disorder.[31] To isolate the feature associated with superconductivity, we subtract this background for each sample using the spectra at the temperature above which the low-bias feature associated with superconductivity disappears (shown as thick lines). The background-corrected conductance spectra ($G_{sub}(V)$ vs V), normalized at high bias, are shown in Figs. 2(g)–2(l). In the $G_{sub}(V)$ vs V spectra, the broadened coherence peaks are visible in all samples. In Fig. 3, we plot the temperature evolution of $G_{sub}(V)$ in the form of an intensity plot (averaged over 32 points, as in Fig. 2), as a function of temperature and bias voltage, for films with different levels of disorder. The lower part of each panel shows resistance vs temperature measured on the same films. For the most ordered film ($T_c \sim 11.9$ K), the features in the tunneling DOS associated with superconductivity disappear at T_c, thereby restoring a flat metallic DOS for $T > T_c$. However, with increase in disorder, the low-bias dip in $G_{sub}(V)$ vs V spectra continues to persist up to a characteristic temperature $T^* > T_c$. The pseudogap temperature T^* remains almost constant for samples with $T_c \lesssim 6$ K. Figure 4 shows the spatial variation of $G_{sub}(V)$ recorded at the lowest temperature along a 150 nm
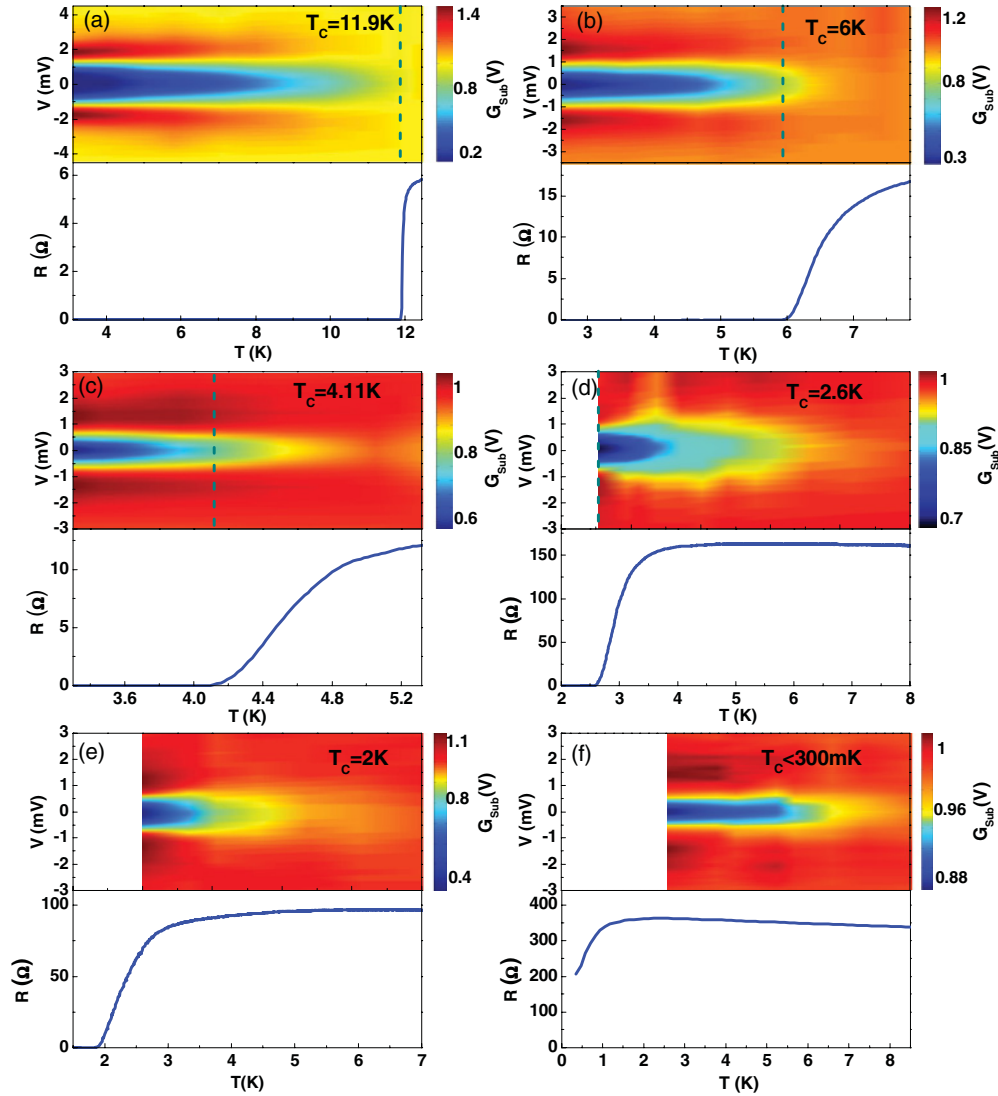
FIG. 3. (Color online) Intensity plots of $G_{sub}(V)$ as a function of temperature and applied bias for six samples (upper part of each panel), along with resistance vs temperature in the same temperature range (lower part of each panel). The vertical dashed lines in the upper panels correspond to T_c.

line for each sample. Although the zero bias dip and the two symmetric peaks are uniform over the entire line for the sample with $T_c \sim 11.9$ K, the superconducting state becomes progressively inhomogeneous with increase in disorder. For the two most disordered samples, for which T_c is smaller than the base temperature of our STM, the local DOS in the pseudogap state shows superconducting domains, a few tens of nanometers in size, separated by regions in which the superconducting feature is suppressed. A similar situation is observed in other samples in the temperature range $T_c < T < T^*$. This is shown in Fig. 5, where we present the spatial variation of $G_{sub}(V)$ at different temperatures for a sample with $T_c \sim 2.7$ K.

Finally, we focus our attention on the magnetotransport properties in the strong disorder limit. Figure 6(a) shows $\rho - H$ at different temperatures for the most disordered film with $k_F l \sim 0.42$. $\rho - H$ shows a pronounced peak at a characteristic field H_p that gradually disappears with increase in temperature. In the most disordered sample, the resistance at 12 T is smaller

than the corresponding zero field value. This peak becomes less pronounced [Figs. 6(b) and 6(c)] as the disorder is reduced and disappears for films with $k_F l > 1$. The peak in $\rho - H$ disappears at a temperature close to T^* for the most disordered sample on which STS was performed [Figs. 6(e) and 6(f)]. For the film with $k_F l \sim 1.23$, which has $T_c \sim 0.6$ K [Fig. 6(d)], ρ increases monotonically with H at 300 mK, exhibiting a broad transition to the normal state as expected for a strongly disordered sample. As expected, for this sample, a positive MR is observed even at $T \gg T_c$, originating from superconducting fluctuations that persist above T_c.

Figure 7 summarizes the evolution of the superconducting state as a function of disorder in the form of a phase diagram, where we plot T_c and T^* as functions of $k_F l$. This phase diagram brings out three distinct regimes of disorder: The intermediate disorder regime (marked as **I**), where the superconducting state is characterized by a single energy scale T_c; the strongly disordered regime (marked as **II**), which is characterized by the emergence of a second energy scale
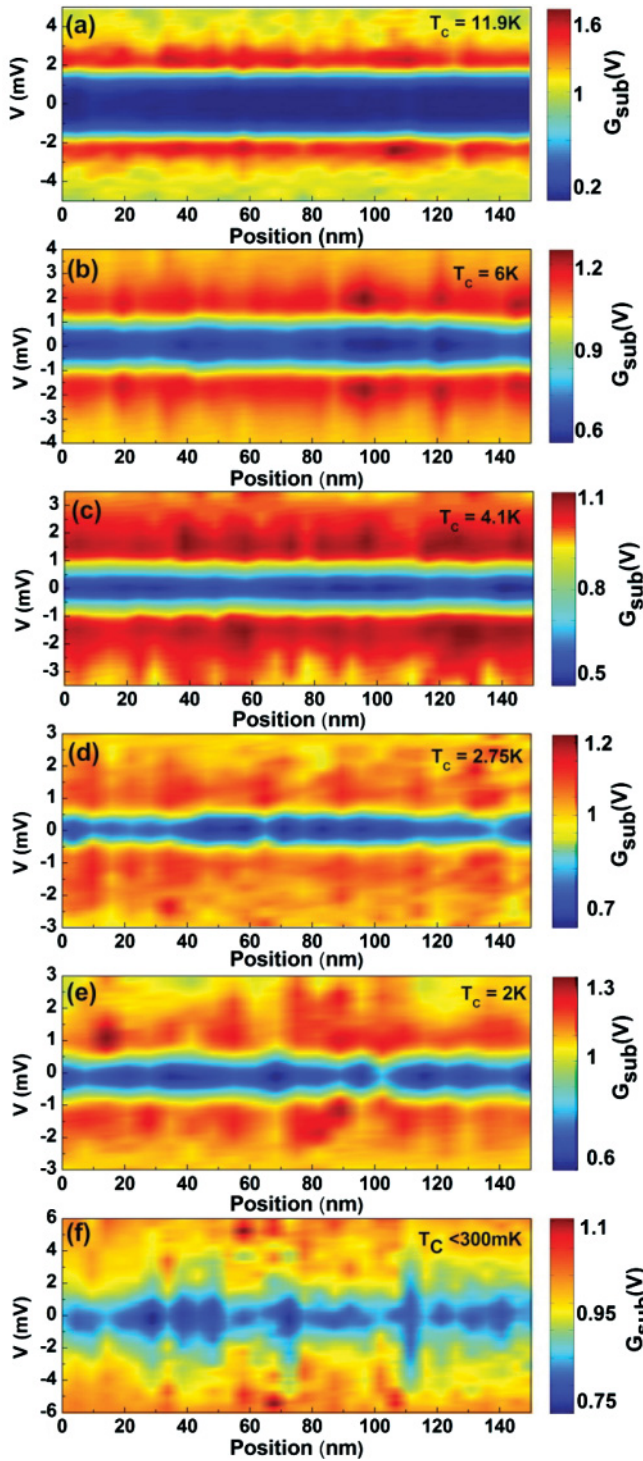
FIG. 4. (Color online) $G_{\mathrm{sub}}(V)$ vs V spectra along a 150 nm line (measured at 2.6 K) for six NbN thin films with different levels of disorder.

FIG. 5. (Color online) Spatial variation of $G_{\mathrm{sub}}(V)$ vs V spectra recorded along a 190 nm line at different temperatures for an NbN thin film with $T_c \sim 2.7$ K. Large inhomogeneity in the tunneling DOS is observed as we enter the pseudogap state.

$T^* > T_c$ up to which the superconducting energy gap persists in the tunneling spectrum; and an even more strongly disordered regime (marked as **III**) ($k_F l < 1$), which does not exhibit any superconducting transition but exhibits a pronounced peak in the MR, which disappears at temperatures close to T^*. In the next section, we discuss the various mechanisms that contribute to these behaviors.
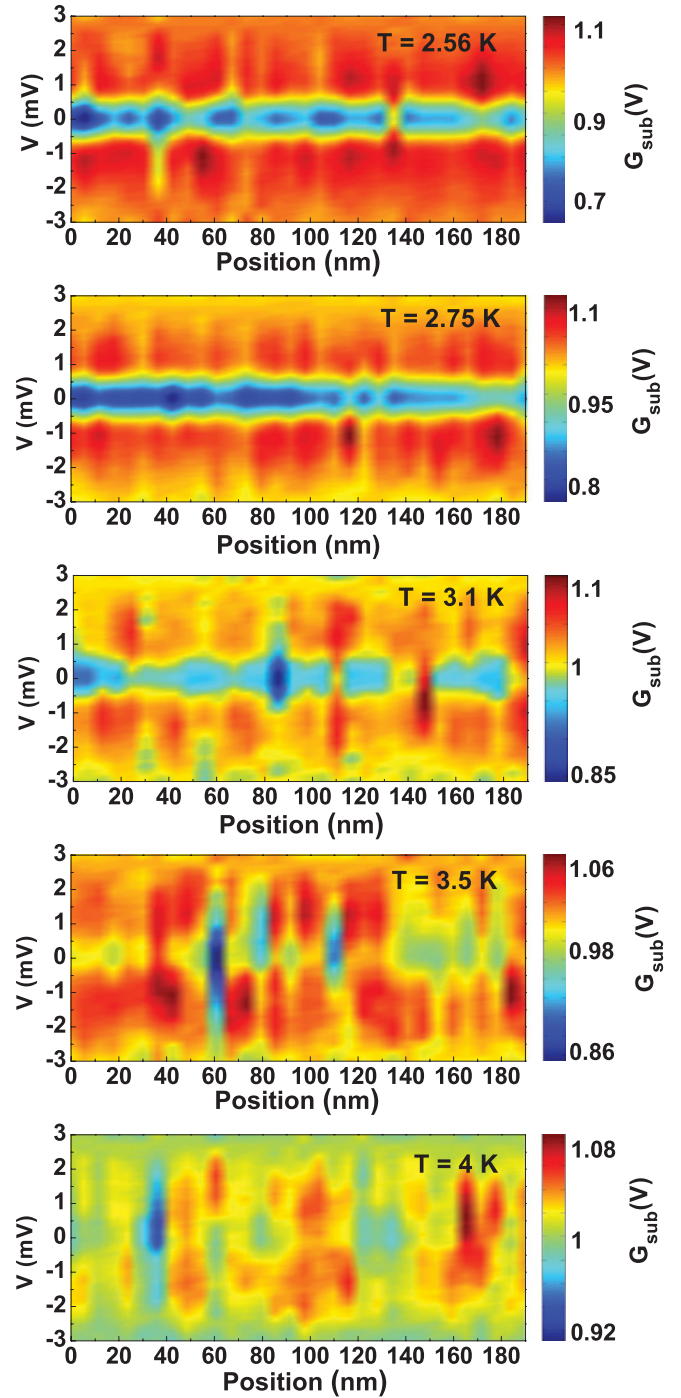
IV. DISCUSSION

Before discussing how different energy scales emerge in a superconductor with increase in disorder, we briefly summarize the mechanisms responsible for the destruction of superconductivity. The superconducting state is characterized by a complex order parameter $\Psi = |\Delta| e^{i\phi}$, where $|\Delta|$ is a measure of the binding energy of the Cooper pairs and ϕ is the phase of the macroscopic condensate. A finite $|\Delta|$ manifests
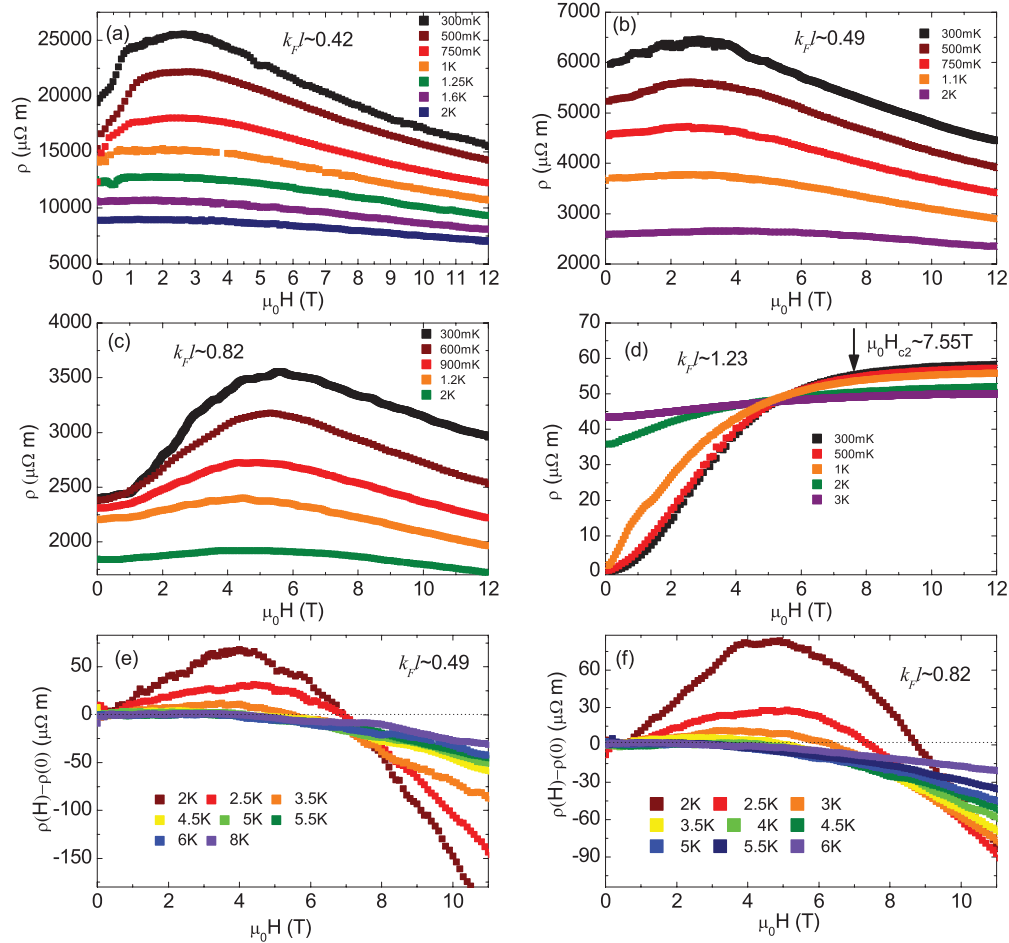
FIG. 6. (Color online) Resistivity as a function of magnetic field at different temperatures for four strongly disordered NbN thin films with (a) $k_F l \sim 0.42$, (b) $k_F l \sim 0.49$, (c) $k_F l \sim 0.82$, and (d) $k_F l \sim 1.23$. The samples with $k_F l < 1$ show a pronounced peak in $\rho-H$. (e) and (f) Expanded view of $\rho(H) - \rho(H = 0)$ vs magnetic field close to temperatures at which the peak in the MR vanishes.

as a gap in the electronic energy spectrum, whereas the zero resistance state results from the phase coherence of the Cooper pairs over all length scales. The first route, through which superconductivity can get suppressed, is by a decrease in $|\Delta|$ caused by a weakening of the pairing interactions. In such a situation, T_c gets suppressed but the superconductor continues to follow conventional BCS behavior, with the superconducting energy gap disappearing at T_c. However, a second, less explored route for the suppression of T_c is through a decrease in the phase stiffness.[22,32] When the phase stiffness becomes sufficiently small, the superconducting state gets destroyed due to a loss of global phase coherence resulting from thermally excited phase fluctuations, leaving pairing amplitude $|\Delta|$ finite above T_c. In such a situation, the superconducting energy gap continues to persist for $T \gg T_c$ until a temperature is reached at which the pairing amplitude also vanishes.

In regime **I** of the phase diagram, T_c monotonically decreases with increase in disorder but continues to follow conventional BCS behavior. Therefore, we expect the decrease in T_c to be caused by a weakening of the pairing interaction. This weakening can result from two effects. First, with increase in disorder, the diffusive motion of the electron results in

an increase in the repulsive *e-e* Coulomb interactions,[19] which partially cancels the phonon-mediated attractive pairing interaction. Some early works attributed the suppression of superconductivity in several disordered superconductors[5,6] solely to this effect.[19,20] The second effect comes from the fact that disorder, in addition to localizing the electronic states close to the edge of the band, increases the one electron bandwidth,[33] thereby decreasing the DOS $N(0)$ close to the middle of the band. Although this effect alone cannot result in the complete suppression of superconductivity, it can have a noticeable effect in the intermediate disorder regime.[34] Both effects are captured at a qualitative level using the modified BCS relation[35] $T_c = 1.13\Theta_D \exp(-\frac{1}{N(0)V-\mu^*})$, where Θ_D is a temperature scale on the order of the Debye temperature, V is the attractive electron–phonon potential, and μ^* is the Coulomb pseudopotential that accounts for the disorder-enhanced *e-e* interactions. Although the available theoretical model on the dependence of the μ^* on disorder in a 3D superconductor is not developed enough to attempt a quantitative fit of our data, the combination of the two effects mentioned previously qualitatively explains the suppression of T_c in regime **I**, where the superconducting energy gap in the tunneling DOS vanishes exactly at T_c.
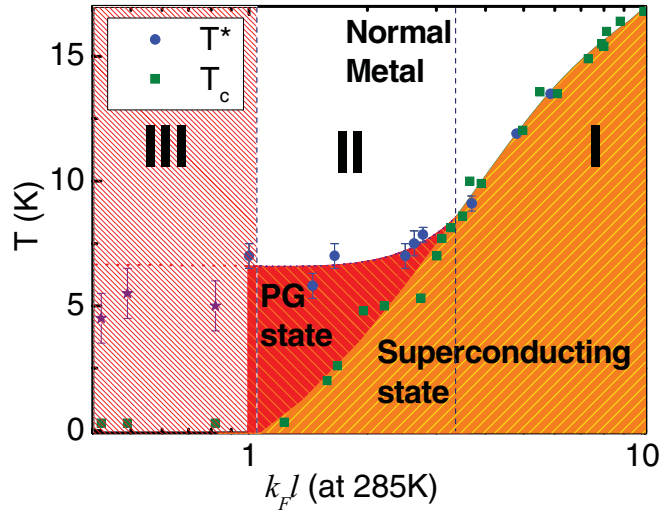
FIG. 7. (Color online) Phase diagram of strongly disordered NbN, showing T_c (green squares) and T^* (blue circles) as functions of $k_F l$. T_c is obtained from transport measurements, while T^* is the crossover temperature at which the low-bias feature disappears from the observed tunneling conductance. The samples with $k_F l < 1$ remain nonsuperconducting down to 300 mK. The three regimes with increasing disorder are shown as **I**, **II**, and **III**. A pseudogap (PG) state emerges between T_c and T^* for samples with $T_c \lesssim 6$ K (regime **II**). The temperature at which the peak in the MR vanishes for the strongly disordered samples (regime **III**) is also shown (purple stars).

As the disorder is further increased, the superconductor enters regime **II**, which is characterized by two temperature scales, namely, T_c, which corresponds to the temperature at which the resistance appears, and T^*, which corresponds to the temperature at which the superconducting energy gap disappears. T_c continues to decrease monotonically with increasing disorder, whereas T^* remains almost constant[36] down to $k_F l \sim 1$, where the superconducting ground state is destroyed. It would be natural to ascribe these two temperature scales to the phase stiffness of the superfluid J and the strength of the pairing interaction $|\Delta|$, respectively. J can be estimated using the relation[22]

$$J = (\hbar^2 a n_s)/(4m^*),\qquad(1)$$

where a is the length scale over which the phase fluctuates and m^* is the effective mass of the electron. A rough estimate of J is obtained from n_s derived from the low-temperature penetration depth[16] $\lambda(T \to 0)$ and setting $a \approx \xi$. In conventional "clean" superconductors, J is several orders of magnitude larger than $|\Delta|$; therefore, phase fluctuations play a negligible role in determining T_c. However, disorder-enhanced electronic scattering decreases n_s, thereby rendering a strongly disordered superconductor susceptible to phase fluctuations. In Fig. 8, we summarize the values of J for NbN films with different T_c estimated from Eq. (1) using experimental values of n_s measured from penetration depth[16] and values of ξ obtained from the upper critical field H_{c2}.[24] Apart from some small numerical factor on the order of one arising from the choice of the cutoff $a \approx \xi$ in Eq. (1), we see that although for the samples in regime **I** $J \gg k_B T_c$ such that phase fluctuations are irrelevant, as we enter regime **II**, J
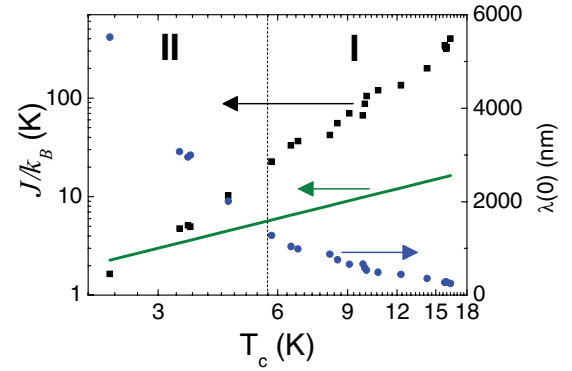

FIG. 8. (Color online) Superfluid stiffness (J/k_B) and penetration depth $\lambda(T \to 0)$ for NbN films with different T_c. The solid line corresponds to $J/k_B = T_c$. Regimes **I** and **II** corresponding to the phase diagram are delineated by the dashed vertical line.

becomes of the order of $k_B T_c$. Moreover, the crossover from regime **I** to regime **II** occurs on the same samples for which we observe a deviation of $n_s(T)$ from the dirty-limit BCS theory, both at zero temperature and finite T.[16] Both effects can be attributed to phase fluctuations in the presence of disorder. As discussed in Ref. 37, as disorder increases, the superfluid stiffness is lower than in the dirty-BCS scenario because the phase of the superconducting order parameter relaxes to accommodate the local disorder, leading to an additional paramagnetic reduction of the superfluid response of the system. At the same time, the enhanced dissipation lowers the temperature scale where longitudinal phase fluctuations can be excited, leading to a linear decrease of $n_s(T)$ in temperature, as observed in our samples.[16] In light of these observations, we conclude that the superconducting state in strongly disordered NbN samples is destroyed at T_c due to phase fluctuations between superconducting domains that are seen to spontaneously form in our STS data (Figs. 4 and 5). However, even above this temperature, $|\Delta|$ remains finite due to phase-incoherent Cooper pairs, which continue to exist in these domains. The relative insensitivity of T^* to disorder and the gradual decrease in T_c suggest that the increase in phase fluctuations is responsible for the decrease in T_c in this regime, while the pairing amplitude remains almost constant. Eventually, at a critical disorder ($k_F l \sim 1$), the superconducting ground state is suppressed by quantum phase fluctuations that are themselves enhanced by disorder. The overall physical picture and the phase diagram obtained in our experiments share many analogies with recent theoretical calculations on disordered superconductors.[34,37,38]

As the disorder is increased further, we enter regime **III**, where all samples remain nonsuperconducting down to 300 mK. This phase is characterized by a peak in MR, which is a hallmark of several strongly disordered superconductors.[9–13] Because the pairing amplitude remains finite down to the critical disorder where $T_c \to 0$, it is expected that superconducting correlations will continue to play a significant role in this regime. The superconducting origin of the MR peak is suggested because it vanishes at temperatures close to T^* measured from STS in samples in regime **II**. Numerical simulations[39] (in two dimensions) also indicate that the nonsuperconducting state could comprise of small

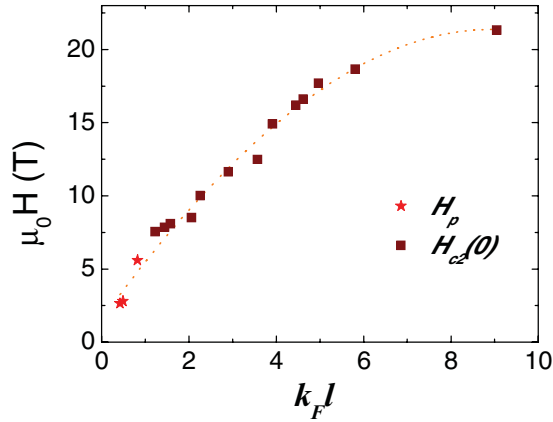FIG. 9. (Color online) Variation of $H_{c2}(0)$ (for $k_F l > 1$) and H_p (for $k_F l < 1$) as a function $k_F l$.

superconducting islands, where quantum phase fluctuations between these islands prevent the establishment of global superconducting order. Such an inhomogeneous scenario[40–42] can give rise to the nonmonotonic variation of $\rho - H$. At low fields, the increase in ρ reflects the gradual decrease in superconducting paths for the current to flow due to the shrinkage in the size of the superconducting droplets. However, at high fields, when the superconducting islands become very small, the superconducting regions are avoided by the current and the decrease in resistance is caused by the gradual increase in normal regions through which the current flows.[43] In such a scenario, H_p is associated with the mean value of the magnetic field where superconducting correlations are almost destroyed in the sample. H_p is therefore expected to evolve smoothly from H_{c2} in the superconducting state as the system enters regime **III** from regime **II**. To verify this, we compare H_p measured at 300 mK for samples with $k_F l < 1$ to $H_{c2}(0)$ for samples with $k_F l > 1$. For the samples with $T_c < 5$ K, $H_{c2}(0)$ is determined from $\rho - H$ scans, at the field where ρ reaches 90% of its normal state value at the lowest temperature of our measurements. For films with higher T_c, $H_{c2}(0)$ was estimated

from the temperature variation of $H_{c2}(T)$ close to T_c, using the dirty-limit formula,[44] $H_{c2}(0) = 0.69 T_c (d H_{c2}/dT)|_{T=T_c}$. Figure 9 shows the evolution of $H_{c2}(0)$ and H_p as a function of $k_F l$. We observe that with increasing disorder, $H_{c2}(0)$ monotonically decreases and smoothly connects to H_p for the samples in regime **III**, providing further confirmation of the superconducting origin of the MR peak.

V. CONCLUSIONS

We have shown how with increase in disorder a 3D conventional superconductor NbN evolves from a BCS superconductor in the moderately clean limit to a situation in which the destruction of the superconducting state is governed by strong phase fluctuations. Based on transport and STS measurements on 3D films spanning a large range of disorder, we construct a phase diagram in which we can identify the dominant interactions in different regimes of disorder: (1) the intermediate disorder regime, where T_c decreases due to a gradual weakening of the pairing interaction; (2) a strongly disordered regime, where T_c is governed by a decrease in the superfluid stiffness, though the pairing strength remains almost constant; and (3) a nonsuperconducting ground state at even stronger disorder, formed of phase-incoherent superconducting puddles/islands. It would be worthwhile to carry out similar measurements on other strongly disordered superconductors such as InO$_x$ or TiN to explore the extent to which such a phase diagram is generic for all disordered s-wave superconductors. It would also be interesting to explore to what extent such a scenario could be applicable to underdoped high-T_c cuprates, which share many similarities with strongly disordered s-wave superconductors.

*pratap@tifr.res.in

[1] P. W. Anderson, J. Phys. Chem. Solid. **11**, 26 (1959).

[2] A. M. Goldman and N. Markovic, Phys. Today **51**, 39 (1998).

[3] A. T. Fiory and A. F. Hebard, Phys. Rev. Lett. **52**, 2057 (1984).

[4] R. C. Dynes, J. P. Garno, G. B. Hertel, and T. P. Orlando, Phys. Rev. Lett. **53**, 2437 (1984).

[5] T. Furubayashi, N. Nishida, M. Yamaguchi, K. Morigaki, and H. Ishimoto, Solid State Comm. **55**, 513 (1985).

[6] G. Hertel, D. J. Bishop, E. G. Spencer, J. M. Rowell, and R. C. Dynes, Phys. Rev. Lett. **50**, 743 (1983).

[7] J. Lesueur, L. Dumoulin, and P. Nedellec, Solid State Comm. **66**, 723 (1988).

[8] K. E. Gray, R. T. Kampwirth, T. F. Rosenbaum, S. B. Field, and K. A. Muttalib, Phys. Rev. B **35**, 8405 (1987).

[9] V. F. Gantmakher, M. V. Golubkov, V. T. Dolgopolov, G. E. Tsydynzhapov, and A. A. Shashkin, JETP Lett. **68**, 363 (1998).

[10] M. Steiner and A. Kapitulnik, Phys. C **422**, 16 (2005).

[11] G. Sambandamurthy, L. W. Engel, A. Johansson, E. Peled, and D. Shahar, Phys. Rev. Lett. **94**, 017003 (2005).

[12] T. I. Baturina, C. Strunk, M. R. Baklanov, and A. Satta, Phys. Rev. Lett. **98**, 127003 (2007).

[13] H. Q. Nguyen, S. M. Hollen, M. D. Stewart Jr., J. Shainline, A. Yin, J. M. Xu, and J. M. Valles Jr., Phys. Rev. Lett. **103**, 157001 (2009).

[14] M. D. Stewart Jr., A. Yin, J. M. Xu, and J. M. Valles Jr., Science **318**, 1273 (2007).

[15] R. Crane, N. P. Armitage, A. Johansson, G. Sambandamurthy, D. Shahar, and G. Grüner, Phys. Rev. B **75**, 184530 (2007).

[16] M. Mondal, A. Kamlapure, M. Chand, G. Saraswat, S. Kumar, J. Jesudasan, L. Benfatto, V. Tripathi, and P. Raychaudhuri, Phys. Rev. Lett. **106**, 047001 (2011).

[17] B. Sacépé, C. Chapelier, T. I. Baturina, V. M. Vinokur, M. R. Baklanov, and M. Sanquer, Nat. Comm. **1**, 140 (2010).

[18] B. Sacépé, T. Dubouchet, C. Chapelier, M. Sanquer, M. Ovadia, D. Shahar, M. Feigel'man, and L. Ioffe, Nat. Phys. **7**, 239 (2011).

[19]P. W. Anderson, K. A. Muttalib, and T. V. Ramakrishnan, Phys. Rev. B **28**, 117 (1983).

[20]A. M. Finkelstein, Phys. B **197**, 636 (1994).

[21]M. Tinkham, *Introduction to Superconductivity* (McGraw-Hill, New York, 1996).

[22]V. J. Emery and S. A. Kivelson, Nature (London) **374**, 434 (1995); Phys. Rev. Lett. **74**, 3253 (1995).

[23]It has also been proposed that when the system is driven into an insulating state by strong disorder, the Cooper pairs can get localized over short length scales, giving rise to an insulating state consisting of localized Cooper pairs: M. V. Feigel'man, L. B. Ioffe, V. E. Kravtsov, and E. A. Yuzbashyan, Phys. Rev. Lett. **98**, 027001 (2007); Ann. Phys. (NY) **325**, 1390 (2010). However, this is beyond the disordered regime explored in this paper.

[24]M. Mondal, M. Chand, A. Kamlapure, J. Jesudasan, V. C. Bagwe, S. Kumar, G. Saraswat, V. Tripathi, and P. Raychaudhuri, J. Supercond. Nov. Magn. **24**, 341 (2011).

[25]S. P. Chockalingam, M. Chand, J. Jesudasan, V. Tripathi, and P. Raychaudhuri, Phys. Rev. B **77**, 214503 (2008).

[26]M. Chand, A. Mishra, Y. M. Xiong, A. Kamlapure, S. P. Chockalingam, J. Jesudasan, V. Bagwe, M. Mondal, P. W. Adams, V. Tripathi, and P. Raychaudhuri, Phys. Rev. B **80**, 134514 (2009).

[27]S. P. Chockalingam, M. Chand, J. Jesudasan, V. Tripathi, and P. Raychaudhuri, J. Phys. Conf. Ser. **150**, 052035 (2009).

[28]M. A. Khodas and A. M. Finkelstein, Phys. Rev. B **68**, 155114 (2003).

[29]Details of our STM are given in Ref. 16.

[30]E. Tousson and Z. Ovadyahu, Solid State Comm. **60**, 407 (1986).

[31]For example, $G(V = 3.7 \text{ mV})/G(0)$ just above T^* increases monotonically from 1.04 to 1.17 as we go across this series from the least disordered sample to the most disordered one.

[32]T. V. Ramakrishnan, Phys. Scr. T **27**, 24 (1989).

[33]J. M. Ziman, *Models of Disorder* (Cambridge University Press, Cambridge, 1979).

[34]A. Ghosal, M. Randeria, and N. Trivedi, Phys. Rev. B **65**, 014501 (2001); Phys. Rev. Lett. **81**, 3940 (1998).

[35]W. L. McMillan, Phys. Rev. **167**, 331 (1968).

[36]Because e-e interactions continue to increase with disorder in regime **II** (e.g., evidenced from a gradual increase in $G(V = 3.7 \text{ mV}) / G(0)$ (Ref. 31) at temperature just above T*), the relative insensitivity of T^* with disorder for samples with $T_c < 6$ K is somewhat counterintuitive. Although we do not have an explanation for this behavior at present, in the absence of e-e interactions, a gradual increase in the spectral gap and its associated temperature scale at strong disorder has been found in the numerical work of Refs. 34 and 39.

[37]G. Seibold, L. Benfatto, C. Castellani, and J. Lorenzana, e-print arXiv:1107.3839 (to be published).

[38]X. T. Wu and R. Ikeda, Phys. Rev. B **83**, 104517 (2011).

[39]K. Bouadim, Y. L. Loh, M. Randeria, and N. Trivedi, Nat. Phys. **7**, 884 (2011).

[40]Y. Dubi, Y. Meir, and Y. Avishai, Phys. Rev. B **73**, 054509 (2006).

[41]For a 3D superconductor–insulator transition deep in the insulating regime, it has been suggested (Ref. 23) that the insulating and the superconducting states could both comprise of Cooper pairs that are delocalized on the superconducting side and localized on the insulating side of the transition. Although such a scenario could also give a MR peak at the pair breaking field (Ref. 42), it is unlikely to be applicable to our samples, which are not deep in the insulating regime.

[42]M. Mueller, e-print arXiv:1109.0245 (to be published).

[43]A similar mechanism for the decrease in resistance at high fields has been proposed in the context of granular superconductors: I. S. Beloborodov, K. B. Efetov, and A. I. Larkin, Phys. Rev. B **61**, 9145 (2000).

[44]N. R. Werthamer, E. Helfland, and P. C. Honenberg, Phys. Rev. **147**, 295 (1966).